A Method for Calculating Near-Infrared-Adjusted Optical Densities for Common Standard Test Charts

Christian Taylor, Amelia Limbocker
Imatest LLC; Boulder, Colorado, USA

Abstract

Near-infrared (NIR) imaging is now prevalent in machine vision, automotive, and biomedical applications, but most step-chart definitions were created for visible imaging. Popular standards assume visible-band weighting and do not account for NIR-sensitive systems. This leads to charts with target densities unoptimized for NIR applications.

We present a methodology for designing NIR test charts whose optical densities (ODs) align with the effective bandpass of a specific camera. First, we model the ISO 5 visual density calculation and the ISO 14524 OECF method for determining density targets for a test chart from spectra of an inkjet print. That method is modified to accept new bandpass weights to accommodate sensitivities not accounted for by ISO 5-3. Three new weights are applied, and reflectance factor density targets are calculated. The results show that target densities shift with alternative spectral weightings, motivating a different NIR chart design.

Introduction

Grayscale test chart patterns are well established as useful tools for evaluating image quality. For many years, they have been employed in various ways. The original grayscales were used to characterize the response of photographic materials to exposure. In 1956, the EIA TV test chart was designed for use with black-and-white TV systems [1]. This pattern incorporated grayscale steps for evaluating gamma and transfer characteristics. By the late 20th century, grayscale charts were a common tool in photography. One of the best-known examples is the Kodak Q-13 / Q-14, which was used for tone reproduction and finding the correct exposure in varied lighting conditions [2]. In 1999, ISO 14524 standardized grayscale OECF charts for digital cameras. The goal of ISO 14524 is to provide a consistent and repeatable way to measure how a digital camera converts light (optical input) to digital numbers (electronic output) [3].

The development of these grayscale tools and charts was driven mainly by the needs of the applications of the time. In 1956, it was for improving the quality of images displayed on televisions. The Kodak charts had utility for photographers and aided proper exposure. By the early 21st century, the focus had shifted to digital photography, where the initial applications largely remained the same: producing higher quality images for human viewing.

As digital imaging sensors became more prevalent, particularly with the advent of smartphones, sensor manufacturing scaled rapidly, and costs declined, enabling new applications. Many new applications and advancements took advantage of the silicon's sensitivity to longer wavelengths of light, specifically between 700-1000 nm [4]. Traditionally, this light was blocked for photographic applications with an IR blocking filter (also known as a hot mirror) [5]. In modern imaging, this NIR light is used in many important applications such as night vision, biometric sensing, automotive monitoring, and machine vision [6] [7] [8].

The relatively recent development of NIR-specific sensing and applications introduces new questions and concerns in the field of image quality testing. Most of the traditional and legacy methods for designing and employing grayscales have mainly, if not exclusively, focused on the human perceptual implications and therefore only considered visible wavelengths of light (380 - 750 nm) [9] [3]. Many properties of a camera system may change between visible and NIR wavelengths, but one of the most crucial is the tone reproduction. The modern standard approach for characterizing tonal reproduction, ISO 14524 and related standards, does not accommodate this change in wavelength and spectral sensitivity [9] [3].

This work examines the relevant ISO standards and proposes a model and method for minimally altering the ISO methods to accommodate NIR testing. ISO 14524 refers to using ISO visual density (ISO 5) in its calculations for specifying test chart design and target densities for a grayscale chart. ISO visual density uses the product of spectral reflectance/transmittance with a weighting function and integration to determine the scalar value of optical density. This weighting does not provide for any integration of light beyond 760 nm [9]. This implies that the ISO visual density used in ISO 14524 does not extend to NIR sensitive applications. We modify the method by replacing the ISO 5 weighting with alternative spectral weights representing different system sensitivities. ISO 14524 is then used to calculate new target densities for test chart designs. The new target ODs are compared against the expected ISO visual weighted target ODs.

Background

ISO 5 gives the definition of density from reflectance as shown in Equation 1. The reflectance measurement and equipment must conform to the geometric conditions outlined in ISO 5 [9].

$$D = -log_{10}(R) \tag{1}$$

Expanding to see the spectrum and including the prescribed weighting function gives us Equations 2 and 3. Where the weighting function is sum normalized and wavelength is sampled in 10 nm increments to match the tabular weighting given in ISO 5-3 [9] [3].

$$D = -log_{10}(\sum_{\lambda} R(\lambda) \cdot W(\lambda)) \tag{2}$$

where,

$$\sum_{\lambda} W(\lambda) = 1 \tag{3}$$

Now that we have density, we can use it to design the grayscale's target densities. This is done according to ISO 14524 [3]. We first need to find the minimum density (D_{min}) and maximum density (D_{max}) for a given print media. This is achieved by

measuring the darkest and brightest patches that can be produced by said print process. Since density is logarithmic, target spacing is defined in terms of equal steps in cube-root luminance ratio [3]. The luminance ratio spanned by print media is

$$\Delta Y = 10^{\,D_{max}-D_{min}} \tag{4}$$

A chart with n patches has the cube-root luminance ratio values defined by linear interpolation between 1 and $\Delta Y^{1/3}$:

$$Y_i^{1/3} = 1 - \frac{i-1}{n-1}\left(\Delta Y^{1/3} - 1\right), \quad i = 1, \dots, n \tag{5}$$

Target densities are then calculated as

$$D_i = log_{10}\left[\frac{\Delta Y}{(Y_i^{1/3})^3}\right] + D_{min}, \quad i = 1, \dots, n \tag{6}$$

ISO 14524 then prescribes a patch order and design geometry for several given values for n [3]. These Equations ensure even spacing of luminance steps perceptually, given the practical constraints of a given print media.

Method

Print Media

To start, we need to collect spectral data for the chosen chart material. For this work, we selected the standard inkjet print process and media used by Imatest to produce reflective matte test charts. A tonal check print is produced by printing every gray tone that can be produced via this process. The file printed contains 64 patches with stepped RGB values from lightest to darkest. To achieve the neutral grays, each of the three channels is the same digital number (DN). For example, R=12, G=12, B=12. For simplicity, we refer to the DN as a single value to represent this, i.e. DN=12. To create the steps, the DN is increased by 8, from DN=0 to DN=252, for a total of 64 steps. The patches are then printed for measurement (Note: The print process includes application of profiling to maintain color accuracy). The spectral reflectance ($R(\lambda)$) of each patch is measured according to the ISO 5 geometry and light source requirements with an Avantes AvaSpec-2048XL spectrometer and a calibrated reference tile. Figure 1 shows $R(\lambda)$ for the 64 patches.

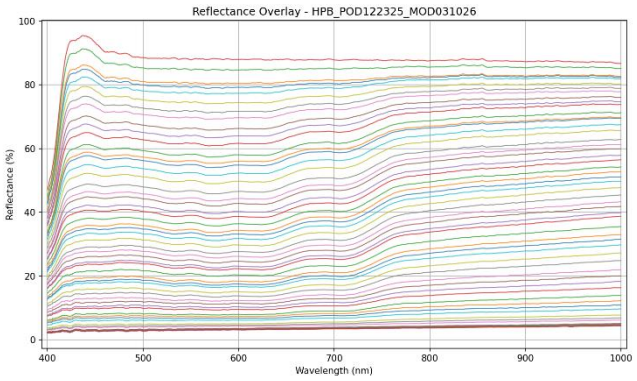

Figure 1. *R(λ) for 64 patches*

ISO Visual Density

To model ISO visual density, a weighting function $W(\lambda)_{ISO}$ is prescribed. We use the 10 nm spacing normalized weighting function in Table 8 of the standard [9]. Figure 2 shows this function

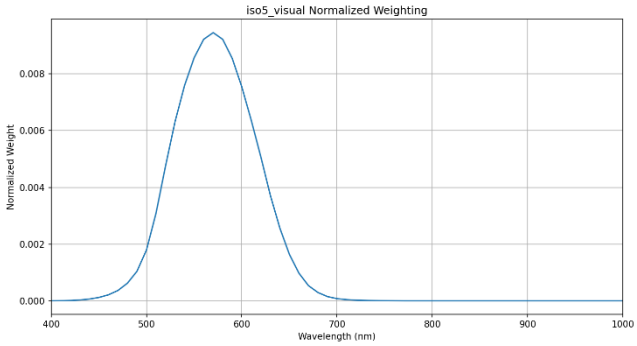

Figure 2. *Normalized ISO 5 Table 8 Weighting function (Weighting is assumed to be 0 at unspecified wavelengths > 760nm)*

We can now calculate the ISO visual density (D_{ISO}) for each of the 64 patches by applying Equation 2 to get:

$$D_{ISO} = -log_{10}\left(\sum \lambda\, R_p(\lambda) \cdot W_{ISO}(\lambda)\right) \tag{7}$$

Figure 3 shows the resulting ISO densities as a function of the input DNs for this print media.

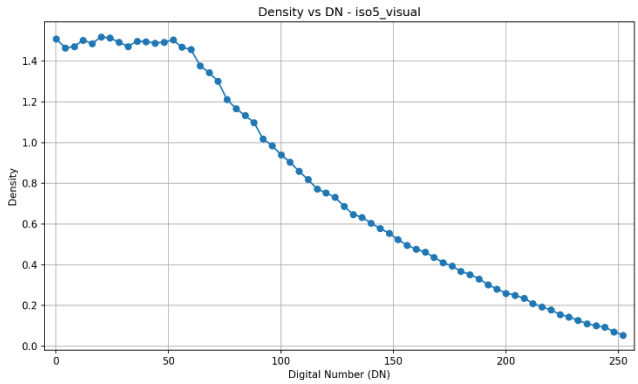

Figure 3. *ISO visual density for 64 reflective inkjet patches*

Now that D_{min} and D_{max} can be determined, ISO 14524 can be employed given Equations 4, 5, and 6. The target densities for this print media are shown in Figure 4.

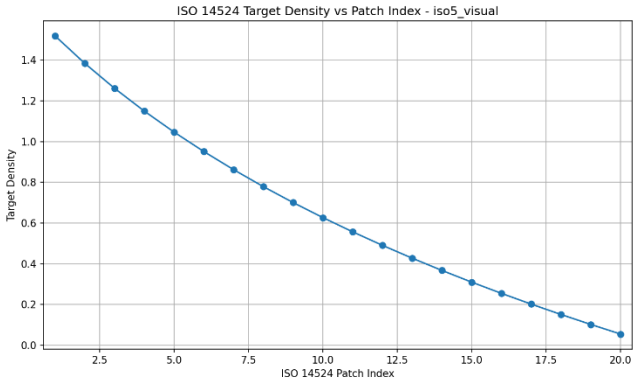

Figure 4. *ISO target densities for 64 reflective inkjet patches*

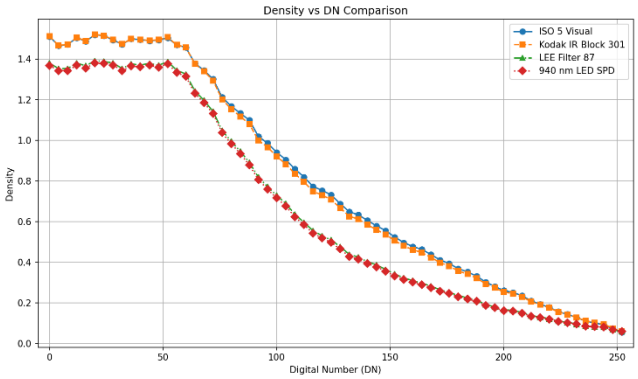

Figure 6. *ISO visual densities and new reflectance factor densities for 64 reflective inkjet patches*

New Spectral Weightings

The same method is used to account for alternate spectral sensitivities with one modification. New weighting functions are used for $W(\lambda)$. In total, we define three new weighting functions to represent plausible real-world applications. One visible dominant weight, one NIR dominant weight, and one application weight. The visible and NIR weights are derived from percent transmission measurements of optical filters, a Kodak no. 301 IR block filter and a Lee no. 87 IR Pass filter respectively. The third weighting was synthesized to model the spectral power distribution of a 940 nm LED light source as an approximation of a plausible automotive in-cabin driver monitoring system. This weight was constructed as a Gaussian distribution with an assumed FWHM of 50 nm with a peak wavelength centered at 940 nm [10] [11]. All new weighting functions are sum-normalized to match the ISO 5 weighting. Figure 5 shows the new normalized weights.

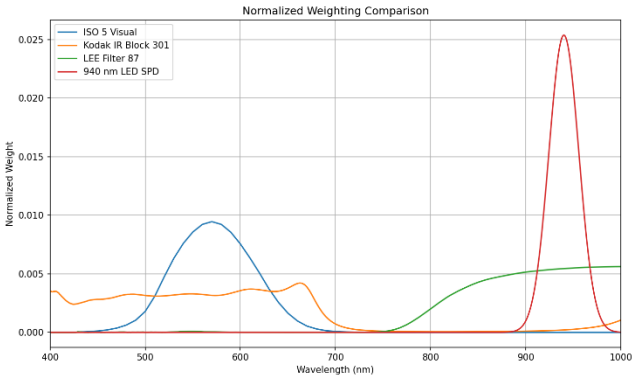

Figure 5. *Sum-normalized candidate spectral weighting functions*

New reflectance factor densities are calculated, given Equation 2, for each of the three new weighting functions for all 64 print patches. These reflectance factor densities are no longer the same as ISO visual densities because they have been calculated with new alternative spectral weighting functions. The three new reflectance factor densities and ISO densities for all patches are shown in Figure 6.

New Target Densities

Target densities can now be calculated according to Equations 4, 5, and 6 using the reflectance factor densities for the new weightings. This is then applied using the same target-density procedure prescribed by ISO 14524 (Note 14524 describes values in the photometric unit of luminance, which is now a misnomer for this method because the spectral weights account for wavelengths beyond the visible spectrum) [3]. This work does not redefine ISO visual density, instead, it applies an analogous reflectance factor density created with varying spectral weights to the ISO 14524 target generation method. The new targets, as well as the ISO visual weighted targets, are shown in Figure 7.

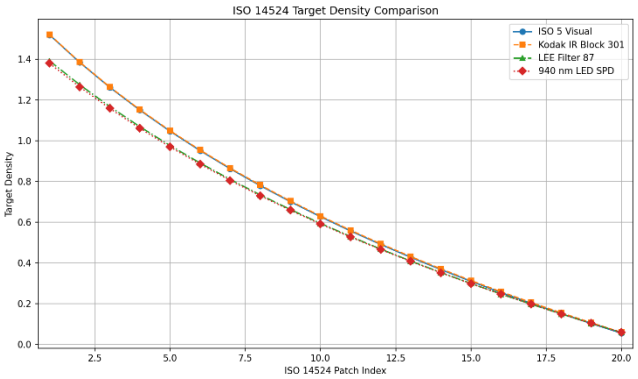

Figure 7. *Target ISO and Reflectance Factor Densities*

Results

We have calculated target densities for our new test chart designs based on ISO visual density and our three new weighting functions. Figure 7 shows clearly that the targets converge at the light end and diverge at the dark end of the scale. Table 1 shows the resulting targets.

Table 1: ISO 14524 Target Densities for All Weights

Patch Index	ISO Visual	Kodak	Lee	940 nm
1	1.519	1.521	1.391	1.379
2	1.384	1.386	1.275	1.263
3	1.262	1.264	1.167	1.158
4	1.150	1.152	1.068	1.060
5	1.047	1.049	0.976	0.969
6	0.951	0.954	0.890	0.884
7	0.862	0.865	0.810	0.804
8	0.779	0.782	0.734	0.729
9	0.700	0.704	0.662	0.658
10	0.627	0.630	0.594	0.591
11	0.557	0.560	0.529	0.527
12	0.490	0.494	0.468	0.466
13	0.427	0.431	0.409	0.407
14	0.367	0.371	0.353	0.351
15	0.310	0.313	0.299	0.297
16	0.254	0.258	0.247	0.246
17	0.202	0.205	0.197	0.196
18	0.151	0.155	0.149	0.149
19	0.102	0.106	0.103	0.103
20	0.055	0.059	0.058	0.058

To illustrate the difference in targets, we calculate the delta of each density at each patch for each weight from the ISO visual targets. These deltas are plotted per patch in Figure 8.

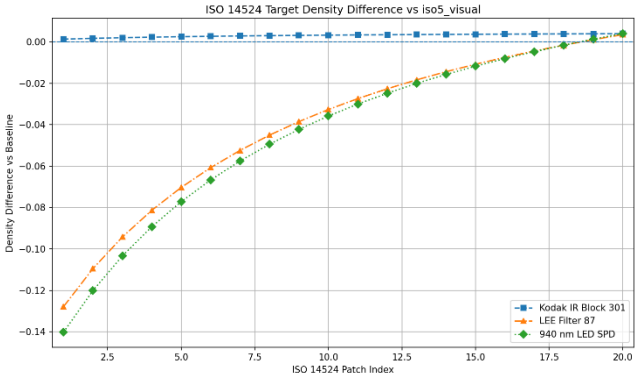

Figure 8. *Target Reflectance Factor Density Deltas from ISO targets*

Several other metrics are calculated to characterize the difference between the new weighting and the ISO standard weighting. The maximum and mean density shift across all patches per weight are shown in Table 2.

Table 2: Comparison of New Weight Targets Against ISO

Weight	Max Absolute Density Shift	Mean Absolute Density Shift
Kodak	0.004	0.003
Lee	0.128	0.041
In-cabin 940	0.140	0.045

Conclusions

Examining the results, we see that there is a meaningful difference between the target densities. Looking at each weighting, we see that the Kodak weighting, which primarily accounts for energy in the visible wavelengths and largely omits NIR wavelengths as seen in Figure 5, shows the smallest differences in targets with a maximum absolute density shift of 0.004. However, the NIR weightings show larger deviations. The Lee weight has a max shift of 0.128 and the modeled 940 weight has a max shift of 0.140.

These results are intuitive when we look at the original spectra for this print process. Figure 1 shows that for these patches, there is a slight increase in reflectance as the wavelength gets longer. This is manifesting in our targets as the darkest patches becoming "brighter" to account for the new D_{max}. This is a key consequence of using alternative spectral weighting. If a system were evaluated using a standard ISO-definition chart despite having NIR sensitivity, the expected D_{max} would be higher than the value effective for the system. We can quantify this difference by solving Equation 1 for the reflectance of the darkest target for both ISO and 940 weights.

$$R = 10^{-D} \tag{8}$$

Using our results, we calculate:

$$R_{ISO} = 10^{-1.519} = 0.0302 \tag{9}$$

And

$$R_{940} = 10^{-1.379} = 0.0418 \tag{10}$$

So, the relative increase is

$$\frac{R_{940}-R_{ISO}}{R_{ISO}} \times 100 = \frac{0.0418-0.0302}{0.0302} \times 100 = 38.4\% \tag{11}$$

This increase of 38.4%, especially for the darkest patch, should be considered seriously for certain applications. The highest density patch is important because it could be used for testing the limit of a given camera system. Some potential implications of this could be that low-light performance may be misunderstood, or ISP tuning or interpretation may be biased because the chart no longer provides the effective signal level assumed by the target densities. Similarly, machine vision detection could also be affected in low-light, an important implication for night vision in-cabin driver monitoring, for example.

Even in examples where the darkest patch shift is not of major consequence, the weights should still be considered. The ISO visual density weight gives no allowance for NIR light [9]. This implies that compliance with the standard does not allow NIR testing. For these modern applications where NIR light is imperative, some testing and benchmarking are crucial. This method offers minimal modifications to the ISO method while allowing for NIR testing, so

a fair comparison can be made between the Visible and NIR performance of digital camera systems.

Limitations

A couple key limitations of this method should be mentioned. The magnitude of the target shift is strongly dependent on the spectral response of the print media. The media chosen for this work has very similar spectral properties in visible and NIR wavelengths. Specifically, the D_{min} and D_{max} do not change by large amounts for the different weights. A much lower D_{max} would produce a substantially different target set.

Another area of caution is in the sophistication of $W(\lambda)$. The weighting functions are an oversimplification of real-world applications. They were chosen for this method to demonstrate possible differences in outcome and should not be assumed to be any real system.

Future Work

As continuation of this work, there are several next steps we will consider. Future work should make the spectral weighting model more sophisticated by defining $W_{sys}(\lambda)$ as the product of a known light source spectral power distribution $(S(\lambda))$, spectral filters $(F(\lambda))$, and quantum efficiency $(QE(\lambda))$ of the sensor to better match a real-world system. A simple model of this could be:

$$W_{sys}(\lambda) \propto S(\lambda)F(\lambda)QE(\lambda) \tag{12}$$

This model could then be used to calculate the targets and to design a chart based on the new weights. Then, printing the different charts and comparing the results of using the mismatched targets with a single camera system. Additional work could include printing the new target sets as physical charts and validating them experimentally.

References

[1] Applied Image, Inc., "QA-70-1 Video Resolution Pattern (EIA-1956) Product Specifications," Rochester, NY.

[2] Kodak, "KODAK Color Separation Guides and Gray Scales," [Online]. Available: https://www.kodak.com/en/motion/page/color-separation-guides-and-gray-scales/. [Accessed December 2025].

[3] International Organization for Standardization, "Photography — Electronic still-picture cameras — Methods for measuring opto-electronic conversion functions (OECFs)," Geneva, 2009.

[4] B. Zhu, "A Review of Image Sensors Used in Near-Infrared and Shortwave Infrared Fluorescence Imaging," *Biosensors,* vol. 14, no. 6, p. 273, 2024.

[5] Active Silicon, "AF-Zoom cameras with IR cut filters," 8 May 2024. [Online]. Available: https://www.activesilicon.com/news-media/news/tech-focus-ir-cut-filters/. [Accessed December 2025].

[6] P. Visconti, R. De Fazio, N. I. Giannoccaro and A. Lay-Ekuakille, "Innovative Driver Monitoring Systems and On-Board Electronics toward Enhanced Vehicle Safety: Technologies, Challenges, and Future Trends," *Sensors,* vol. 25, no. 2, p. 562, 2025.

[7] S. Farokhi, J. Flusser and J. Kittler, "Near infrared face recognition: A literature survey," *Computer Science Review,* vol. 21, pp. 1-17, 2016.

[8] M. S. Millán and J. Escofet, "Fabric inspection by near-infrared machine vision," *Optics Letters,* vol. 29, no. 13, pp. 1440-1442, 2004.

[9] International Organization for Standardization, "Photography — Density measurements — Part 3: Spectral conditions," Geneva, 1995.

[10] ams-OSRAM AG, "SFH 4047 Datasheet," ams-OSRAM AG, 2023.

[11] ams-OSRAM AG, "SFH 47278BS A01 Datasheet," ams-OSRAM AG, 2025.

Author Biography

Christian Taylor received his BS in Imaging Science from Rochester Institute of Technology (2015). He has worked at Imatest in Boulder, Colorado since 2016 and currently holds the role of Chief Product Officer.

Amelia Limbocker received her BFA in Photography with a minor in English from Virginia Intermont College (2014), and a BS in Photographic and Imaging Science with a minor in Imaging Systems from Rochester Institute of Technology (2016). She currently works as an Imaging Science Engineer at Imatest, designing custom charts, providing chart recommendations, and ensuring chart quality.